Towards Fine-Grained Indoor White Space Estimation

***Abstract*—Exploring white spaces in the indoor environment has been recognized as a promising way to satisfy the rapid growth of the wireless spectrum demand. Although a few indoor white space exploration systems have been proposed in the past few years, they mainly focused on exploring white spaces at a small set of candidate locations. However, what we need are the white space availabilities at arbitrary indoor locations instead of only those at the candidate locations. In this paper, we first perform an indoor TV spectra measurement to study the characteristics of indoor white spaces in a fine-grained way. Then, we propose a Fine-gRained Indoor white Space Estimation mechanism, called FRISE, which could accurately estimate the white space availabilities at arbitrary indoor locations. FRISE mainly consists of a method to determine the positions of candidate locations and an accurate spatial interpolation algorithm. Furthermore, we evaluate the performance of FRISE based on real-world measured data. The evaluation results show that FRISE outperforms the existing methods in estimating white spaces at arbitrary indoor locations.**

I. Introduction

The fast growth of the mobile devices and applications has led to the increasing demand of wireless spectra for communication. Unfortunately, the amount of unlicensed wireless spectra that are free to use is very limited, while most of the licensed spectra are underutilized [1]. Facing the shortage of the wireless spectra, the concept of Dynamic Spectrum Access (DSA) was proposed to improve the wireless spectrum utilization.

In 2008, the Federal Communication Commission (FCC) issued the rule that allows unlicensed devices to access locally unoccupied TV spectra, which are usually referred to as TV white spaces [2]. After that, the unlicensed use of TV spectra became a popular application of DSA [3], [4]. Although the unlicensed use of TV white spaces is allowed, FCC also requires that unlicensed devices should not interfere with any of the licensed TV transmissions. Therefore, all user devices (especially the unlicensed ones) should get the spectrum's availability information before accessing it.

FCC proposed a geo-location database approach [5], [6] to protect the licensed TV transmissions, which requires the unlicensed users to query a geo-location database in order to obtain the white space availability at outdoor locations. However, in the indoor environment, there exist more white spaces than the outdoor scenarios because of the existence of the indoor obstacles (e.g., walls) [7]. Since the geo-location database approach does not consider the signal attenuation caused by indoor obstacles, directly applying it to the indoor environment would lead to a too conservative result.

In 2013, Ying et al. [7] studied the characteristics of indoor white spaces, and proposed the first indoor white space exploration system, namely WISER. Then, different methods were proposed to boost the performance of indoor white space exploration [8], [9]. The existing indoor white space exploration systems aim at constructing an indoor white space availability map, which indicates the availabilities of the TV spectra at different indoor locations. Users could submit their indoor locations, and then receive the corresponding list of white spaces according to the current indoor white space availability map. The construction of the indoor white space availability map can be divided into two steps: *recovery at candidate locations* and *estimation at arbitrary locations*.

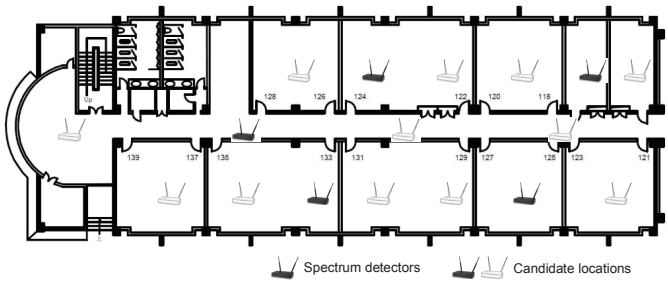

Fig. 1. Model of indoor white space exploration

Step I Recovery at candidate locations: In order to construct the indoor white space availability map, as shown in Fig. 1, a set of candidate locations should be selected to cover every of the rooms and corridors. Due to limitations on budget and runtime cost, existing approaches turn to carefully deploying a certain number of spectrum detectors at a part of the candidate locations, and then recover the status of TV spectra at the other candidate locations based on indoor spectrum's characteristic of spatial-spectral correlations.

Step II Estimation at arbitrary locations: Constructing the indoor white space availability map needs the signal strengths of TV spectra at arbitrary indoor locations, and then compare them with a white space threshold to determine the availability distribution. Given the signal strengths at candidate locations, the signal strengths at arbitrary indoor locations are estimated based on some spatial interpolation method.

However, the existing works could not perform Step II in an accurate enough way, the details of which are reflected in the following two aspects: (A) there lacks a method to determine the positions of candidate locations, and (B) the spatial interpolation method is not accurate enough. All existing works assume that the positions of candidate locations are given beforehand. Whereas our experiment results in Section II demonstrate that different positions of candidate locations would lead to different performances of estimation. This gives the motivation for a method to determine the positions of the candidate locations. Furthermore, existing works apply a kind of constant spatial interpolation to do the estimation. The constant interpolation considers the vicinity of a candidate location share the same signal strengths of TV spectra with the candidate location. We have also shown that directly applying the constant interpolation approach would lead to high error rates of estimation.

Unfortunately, it is difficult to solve the above two problems. The first challenge is determining the positions of candidate locations. In this process, we should select a set of locations that make the estimation at arbitrary locations as accurate as possible. A simple way to determine the positions is selecting a set of locations to collect the training data, and choose a subset of them based on an enumeration way to maximize the estimation accuracy. However, the number of possible sets of training locations is exponential, which makes it impossible to do exhaustive enumeration. Moreover, the locations without training data can also be considered, meaning that all possible locations should be able to be considered as a candidate location. The other challenge is accurate spatial interpolation. Different from the constant interpolation, an accurate spatial interpolation method must take the correlations of different locations into consideration. However, it is difficult to obtain the precise correlations between an arbitrary pair of locations, since we could not get the training data at any of the locations.

In this paper, we propose FRISE, which is a Fine-gRained Indoor white Space Estimation mechanism. In response to the first challenge, FRISE uses mutual information [10] to describe the "importance" of each of the indoor locations. Since the mutual information is independent to the detailed measurement values, we could describe the "importance" of arbitrary indoor locations instead of only those with training data. Besides, we determine the positions of candidate locations in sequence, and iteratively choose the most "important" locations. In this way, the position determination could be achieved in polynomial time. For the second challenge, we build a Gaussian process model for the signal strengths at arbitrary locations, the kernel function of which could approximately describe the correlations between any pair of locations. Besides, the spectral and temporal correlations are also considered to improve the performance of the interpolation. The main contributions of this paper are summarized as follows:

- We perform indoor TV spectra measurement in a lab room and a corridor. The measurement results demonstrate the influence of different positions of candidate locations and the inaccuracy of the constant interpolation, which motivates this work.
- FRISE improves the accuracy of estimation at arbitrary locations by first determining the proper positions of candidate locations and then applying an accurate spatial interpolation method to do the estimation. To the best of our knowledge, FRISE is the first mechanism that study the position determination of candidate locations.
- We evaluate the performance of FRISE with extensive real-world measured data. The evaluation results demonstrate that FRISE leads to a maximum 38.5% less white space error compared to the constant interpolation and 47.0% less white space error compared to the random determination for positions of candidate locations.

The rest of the paper is organized as follows. In Section II, we present our indoor TV spectra measurement experiment. Then we propose detailed system design of FRISE in Section III. In Section IV, we evaluate FRISE. Related works and conclusions are given in Section V and Section VI, respectively.

II. Indoor TV spectra Measurement

In this section, we present our indoor TV spectra measurement. Different from the existing TV spectra measurement, which measured the TV spectra only at the candidate locations, we measure the TV spectra in a more fine-grained way. The measurement is carried out in two typical indoor environments: a lab room (abbr. $10m \times 45m$) and a long corridor (abbr. $120m$ long), the maps of which are shown in Fig. 2. The purpose of the measurement is to analyze the performance of the constant interpolation as well as the influence of positions of candidate locations to the TV spectra estimation. The measurement observations demonstrate the necessity to a fine-grained indoor white space estimation mechanism.

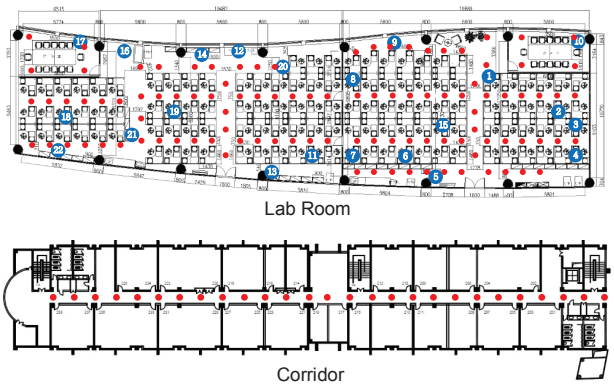

Fig. 2. Map of the lab room and corridor.

A. Equipment and Setup

Our measurement device consists of a USRP N210, a log periodic PCB antenna, and a laptop. The USRP N210 is equipped with the SBX daughter-board with 5-10 dBm noise figure. We measure 56 UHF digital TV channels between 470 MHz - 566 MHz and 606 MHz - 958 MHz with 8 MHz channel bandwidth.

Just the same as the prior works [7], [8], we implement an energy detector to detect the existence of signal transmissions. The energy detector is based on the fast Fourier transform (FFT) with bin size 1024 and sample rate 4 MHz. The signal strength of a channel is calculated by averaging the value in the corresponding bins. We can get the status of a channel by comparing its signal strength with a preset threshold. If the signal strength of the channel is greater than the threshold, this channel is occupied, otherwise we consider it vacant. We use a threshold of -84.5 dBm/8 MHz, which is determined using the same way as [7], [8]. Although the threshold is higher than that suggested by FCC, which is -114 dBm/8 MHz, we set the threshold in this way due the device limitation. Since the -84.5 dBm/8 MHz threshold is also utilized by prior works, we believe that it is feasible in our TV spectra measurement and analysis.

The TV spectra measurement can be divided into two parts: synchronous measurement and asynchronous measurement.

B. Synchronous Measurement

In the synchronous measurement, we deploy 22 measurement devices in the lab room (blue points in Fig. 2) and continuously measure the signal strengths of TV channels for a period of 2 weeks (Dec. 28, 2015 - Jan. 10, 2016). The measurement devices are calibrated using a RF signal generator and synchronized using "crontab" of Ubuntu 12.04.

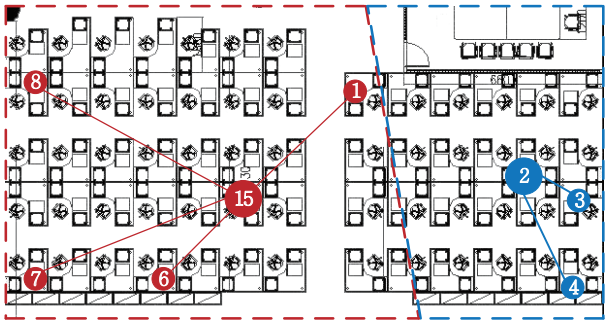

Fig. 3. Example of constant interpolation.

TABLE I
PERFORMANCE ANALYSIS ABOUT CONSTANT INTERPOLATION

Candidate locations	15				2	
Locations	1	6	7	8	3	4
# of errors	4.5	8.8	6.8	6.3	5.7	9.1
White space error	8%	16%	12%	11%	10%	16%

We synchronously measure the signal strengths of 56 TV channels every 5 minutes in the two weeks period. The observations are as follows:

1) The constant interpolation could not accurately estimate the status of TV channels: The constant interpolation is commonly utilized by the existing indoor white space exploration systems to estimate the status of TV channels at arbitrary indoor locations. However, no one has analyzed its performance. Hence, we analyze the performance of the constant interpolation based on the measurement results. We first give a simple example. Fig. 3 shows a part of the lab room, which contains the measurement locations 1, 2, 3, 4, 6, 7, 8, and 15. We choose location 2 and 15 as the candidate locations. If we apply the constant interpolation to do the estimation at arbitrary locations, then the status of TV channels at location 3 and 4 are considered the same as location 2, while the status of TV channels at location 1, 6, 7, and 8 are considered the same as location 15. We compare the real status of the 56 TV channels with the estimated values at each time slot (5 minutes), and calculate the average errors of the estimation. Here we denote the *white space error* as the ratio between the number of channels whose status are incorrectly estimated and the total number of channels. We give the detailed definition of white space error in Section IV-A. The results are shown in TABLE I. For instance, at location 1, the status of an average of 4.5 channels are incorrectly estimated, which is about 8% of the 56 channels. At location 4, about 16% of the channels (9.1) are estimated to wrong status.

We then analyze the performance of constant interpolation based on all the measured data. Specially, we set location 15 and 19 as the candidate locations, and compare the real status of TV channels at the other 20 locations with those estimated using the constant interpolation. The average number of incorrectly estimated channel over all the remaining 20 locations is 8.52, which leads to an average white space error of 15.2%. This means that an average 15.2% of the TV channels would be incorrectly identified if we apply the constant interpolation method. This white space error (15.2%) make constant interpolation not accurate enough, and thus it is essential to design an accurate algorithm to do the estimation at arbitrary locations.

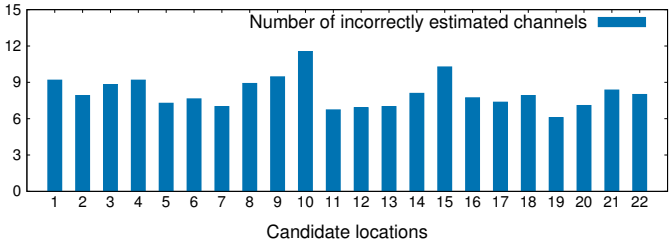

Fig. 4. Influence of positions of candidate locations.

2) Different positions of candidate locations lead to different performances of estimation: We also observe that different positions of candidate locations would lead to different performances of the estimation at arbitrary locations. Here, we first set location 1 as the candidate location, and calculate the average number of channels whose status are incorrectly estimated over the remaining 21 locations. Then, we set location 2, 3, ..., 22 as the candidate location in sequence, and compare the performance of estimation under different candidate locations. The results are shown in Fig. 4. The y-axis refers to the average number of incorrectly estimated channels under different candidate locations. For instance, when we use location 1 as the candidate location, the status of an average of 9.18 channels are incorrectly estimated at the remaining 21 locations. It is observed that when the positions of the candidate locations are different, the number of incorrectly estimated channels are also different, which leads to different estimation performances. Hence, it is important for us to determine a proper set of positions for candidate locations in order to get a higher estimation accuracy.

3) There exist spatial-spectral-temporal correlations among TV spectra: We then study the correlations of TV spectra between different locations, channels, and time slots, which we call spatial-spectral-temporal correlations. Although the spatial and spectral correlations have been studied by prior works [7], [8], we still get some new observations.

We focus on the spatial correlation in a room or corridor, instead of that between different rooms or corridors, which is already studied. Based on the measured data, we get a vector for each measured location that contains the signal strengths of all TV channels over the two weeks interval. Then we calculate the Pearson product-moment correlation coefficients [11] of all pairs of locations, and draw Fig. 5(a) based on the result. Pearson product-moment correlation coefficient is widely used as a measure of the linear dependence between two variables, the value of which is between -1 and 1 where 1 is total positive correlation and -1 refers to total negative correlation. In Fig. 5(a), we observe that most of the location pairs have relative large Pearson product-moment correlation coefficients, which means the 22 measured locations in the lab room are tightly correlated. If the spatial correlation could be utilized into the estimation at arbitrary locations, we believe that its accuracy would be improved. Our observations on spectral correlation are similar to prior works, which is shown in Fig. 5(b). A channel may be tightly correlated with some channels while almost independent to others. Thus, it would be a good way to cluster all the TV channels into several groups, and only consider the correlations in the same group. This property

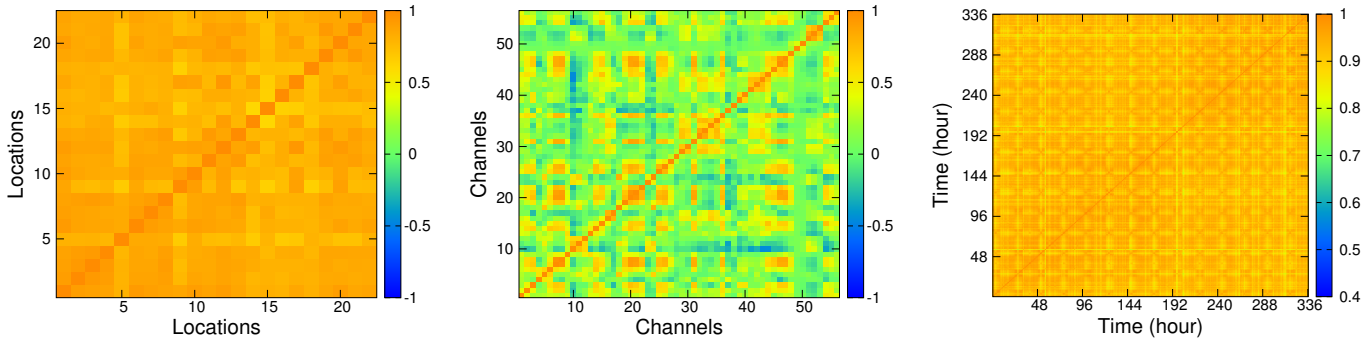

(a) Spatial correlation (b) Spectral correlation (c) Temporal correlation

Fig. 5. Correlations of indoor TV spectra.

would help us to speed up our spatial interpolation method, the details of which are discussed in Section III-D.

Furthermore, we also study the temporal correlation of TV spectra while existing works on indoor white space exploration mainly focus on the spatial and spectral correlations. Fig. 5(c) illustrates the Pearson product-moment correlation coefficients between different time slots in the two weeks interval. In order to give a clear result, we change the range of Pearson product-moment correlation coefficients to [0.4,1] here. We observed that the temporal correlation shows the periodical property. For some time slots, they may have relatively small Pearson product-moment correlation coefficients with their neighbors but be tightly correlated with the time slots which are one period after or before them. The temporal correlation could help us simplify the process of training FRISE, because we do not need to synchronously measure the TV spectra in the training process. The details are shown in Section III-D.

C. Asynchronous Measurement

In order to propose an accurate algorithm to estimate TV spectra at arbitrary locations, we should study the indoor TV spectra in a fine-grained way, which means that we should deploy the measurement devices in the indoor environment as dense as possible. However, due to the limitation of budget, we do not have enough measurement devices to support a synchronous fine-grained measurement. We instead apply an asynchronous way to do the measurement.

We choose two typical indoor environments, the lab room and a long corridor, to do the measurement. We measure the TV spectra at the same lab room with the synchronous measurement, and choose 105 locations (red points in room of Fig. 2). We mount our measurement device on a cart, and measure all the TV channels at one location after another. We also record the time after every measurement. In the long corridor, we choose 27 locations (red points in the corridor of Fig. 2) and perform the measurement in the same way. Every day we perform one round of measurement. The asynchronous measurement lasts for a period of two weeks.

The observations of the asynchronous measurement are similar with the synchronous measurement. Actually, the asynchronous measurement presents an efficient way to train FRISE, because in the real training process, it is impractical that we deploy a lot of spectrum detectors and synchronously measure the TV channels at different indoor locations.

III. System Design

This section shows the design of FRISE. At first, we give an overview of FRISE. Then, we describe the implementation of the multitask Gaussian process based spatial interpolation. After that, we introduce the mutual information based method to determine the positions of candidate locations. At last, we introduce some methods to speed up FRISE.

A. System Overview

The indoor white space exploration systems aim at constructing an indoor white space availability map, which indicates the white space availabilities of the whole indoor environment. The construction of the map could be divided into two steps: recovery at candidate locations (Step I) and estimation at arbitrary locations (Step II). Existing works mainly focus on Step I. They assume that a set of candidate locations are given in advance, and try to select a part of candidate locations to deploy spectrum detectors. Based on the measurement results of spectrum detectors, the signal strengths of TV spectra at all candidate locations could be accurately recovered.

Given the signal strengths at all candidate locations, FRISE aims at estimating those at arbitrary locations (Step II) in a more accurate way. FRISE improves the accuracy of the estimation in two ways:

- FRISE first applies a mutual information based method to determine the proper positions of candidate locations.
- FRISE further use a multitask Gaussian process based spatial interpolation by considering the spatial-spectral-temporal correlations among TV spectra.

We have to note that in this work, we focus on improve the accuracy of estimation at arbitrary locations, and do not consider the errors in the recovery at candidate locations. Building a system which jointly consider the errors of Step I and Step II is one of our future work.

Since the algorithm to determine the positions of candidate locations is based on the estimation results, in the following parts, we first assume the positions of candidate locations are given and describe the multitask Gaussian process based spatial interpolation algorithm. Then we present the algorithm to determine the positions of candidate locations.

B. Multitask Gaussian Process Based Spatial Interpolation

Gaussian process regression is a Bayesian modeling technique that has been widely used for various realms, such as

machine learning [12], sensor reading prediction [13], [14], and time-series analysis [15]. Compared to the commonly used linear regression, the Bayesian nature Gaussian process could give us the extra uncertainty about the estimations. In addition, the noise of measurement could also be considered in the Gaussian process model.

Gaussian process is usually used to predict a single output (or task) based on one or more inputs. However, there exist dozens of TV channels with correlations. If we simply train a Gaussian process model independently for each channel, we would "waste" the correlations among channels. Hence, we explore a multitask Gaussian process regression model [16], [17], which estimates the signal strength of some channel not only based on the same channel's information, but also based on the signal strengths of other correlated channels.

Given the set of N inputs $\boldsymbol{x}_1, \boldsymbol{x}_2, \ldots, \boldsymbol{x}_N$ with $\boldsymbol{x}_i = (p_i, q_i, t_i)^T$ where (p_i, q_i) is the coordinate of the an location, and t_i refers to the time. The corresponding signal strengths of TV channels are defined as

$$\boldsymbol{y} = (y_1^1, \ldots, y_N^1, y_1^2, \ldots, y_N^2, \ldots, y_N^M), \tag{1}$$

where y_i^ℓ is the signal strength of the ℓth TV channel at location (p_i, q_i) when the time is t_i. Here M refers to the number of TV channels.

According to the Gaussian process theory [12], [16], $\boldsymbol{y}$ can be assumed to obey a multivariate Gaussian joint distribution with a mean value 0, which means that

$$\boldsymbol{y} \sim \mathcal{N}(\boldsymbol{0}, K), \tag{2}$$

where K is the covariance matrix. The covariance matrix K is defined by a kernel function $k(\boldsymbol{x}_i, \boldsymbol{x}_{i'}, \ell, \ell')$ which refers to the covariance between two observations y_i^ℓ and $y_{i'}^{\ell'}$. Actually, it is the kernel function $k(\boldsymbol{x}_i, \boldsymbol{x}_{i'}, \ell, \ell')$ that related one observation (here is the signal strength) to another. According to the multitask Gaussian process theory [16], $k(\boldsymbol{x}_i, \boldsymbol{x}_{i'}, \ell, \ell')$ can be rewritten as

$$k(\boldsymbol{x}_i, \boldsymbol{x}_{i'}, \ell, \ell') = K^c_{\ell\ell'} k^x(\boldsymbol{x}_i, \boldsymbol{x}_{i'}), \tag{3}$$

where K^c is an $M \times M$ positive semi-definite matrix that specifies the spectral correlation and k^x is a covariance function which describes the spatial-temporal correlations. $K^c_{\ell\ell'}$ is the element at ℓth row and ℓ'th column of K^c, which refers to the correlation between channel ℓ and ℓ'. If we let

$$K^x = \begin{bmatrix} k^x(\boldsymbol{x}_1, \boldsymbol{x}_1) & k^x(\boldsymbol{x}_1, \boldsymbol{x}_2) & \cdots & k^x(\boldsymbol{x}_1, \boldsymbol{x}_N) \\ k^x(\boldsymbol{x}_2, \boldsymbol{x}_1) & k^x(\boldsymbol{x}_2, \boldsymbol{x}_2) & \cdots & k^x(\boldsymbol{x}_2, \boldsymbol{x}_N) \\ \vdots & \vdots & \ddots & \vdots \\ k^x(\boldsymbol{x}_N, \boldsymbol{x}_1) & k^x(\boldsymbol{x}_N, \boldsymbol{x}_2) & \cdots & k^x(\boldsymbol{x}_N, \boldsymbol{x}_N) \end{bmatrix},$$

with $K^x \in \mathbb{R}^{N \times N}$. The covariance matrix K in equation (2) can be denoted as

$$K = K^c \otimes K^x, \tag{4}$$

where $\otimes$ refers to the Kronecker product [18]. This means that K is an $MN \times MN$ matrix.

Given the signal strengths of TV channels at the candidate locations, that is $\boldsymbol{y}$, we try to estimate the signal strengths of arbitrary indoor locations. For example, if we want to know the signal strength of channel ℓ at location (p_*, q_*) when the time is t_*, where the corresponding input is $\boldsymbol{x}_* = (p_*, q_*, t_*)^T$, we have the following results

$$\begin{bmatrix} \boldsymbol{y} \\ y_*^\ell \end{bmatrix} \sim \mathcal{N}\Big(\boldsymbol{0}, \begin{bmatrix} K & (K_*^\ell)^T \\ K_*^\ell & K_{**}^\ell \end{bmatrix}\Big), \tag{5}$$

with

$$K_{**} = k(\boldsymbol{x}_*, \boldsymbol{x}_*, \ell, \ell) = K^c_{\ell\ell} k^x(\boldsymbol{x}_*, \boldsymbol{x}_*), \tag{6}$$

and

$$K_*^\ell = K_\ell^c \otimes K_*^x, \tag{7}$$

where K_ℓ^c is the ℓth column of K^c, and K_*^x is the vector of covariances between $\boldsymbol{x}_*$ and the input $\boldsymbol{x}_1, \boldsymbol{x}_2, \ldots, \boldsymbol{x}_N$,

$$K_*^x = [k^x(\boldsymbol{x}_*, \boldsymbol{x}_1), k^x(\boldsymbol{x}_*, \boldsymbol{x}_2), \ldots, k^x(\boldsymbol{x}_*, \boldsymbol{x}_N)]^T. \tag{8}$$

The probability distribution of y_*^ℓ given the observations $\boldsymbol{y}$ is a Gaussian [12], [14]:

$$y_*^\ell | \boldsymbol{y} \sim \mathcal{N}(K_*^\ell K^{-1} \boldsymbol{y}, K_{**}^\ell - K_*^\ell K^{-1} (K_*^\ell)^T). \tag{9}$$

We use the mean value

$$\bar{y}_*^\ell = K_*^\ell K^{-1} \boldsymbol{y} \tag{10}$$

as the estimation of y_*^ℓ, and the variance

$$\text{var}(y_*^\ell) = K_{**}^\ell - K_*^\ell K^{-1} (K_*^\ell)^T \tag{11}$$

as the uncertainty of the estimation.

The mean value $\bar{y}_*^\ell$ and variance $\text{var}(y_*^\ell)$ rely on the values of K, K_*^ℓ, K_{**}^ℓ. According to their definitions, if we find the expression of the kernel function $k(\boldsymbol{x}, \boldsymbol{x}_{i'}, \ell, \ell')$, the values of K, K_*^ℓ, K_{**}^ℓ can be easily obtained. As shown in equation (3), the kernel function can be expressed as the product of two parts: $K^c_{\ell\ell'}$ and $k^x(\boldsymbol{x}_i, \boldsymbol{x}_{i'})$, where K^c is the matrix referring to the spectral correlation, and k^x is the spatial-temporal kernel. We study their expressions one by one.

The matrix K^c is required to be positive semi-definite [16]. A common parametrization to guarantee positive-semidefiniteness of K^c is to use the Cholesky decomposition $K^c = LL^T$, where L is a lower triangular matrix

$$L = \begin{bmatrix} \theta_{11}^c & 0 & \cdots & 0 \\ \theta_{21}^c & \theta_{22}^c & \cdots & 0 \\ \vdots & \vdots & \ddots & \vdots \\ \theta_{M1}^c & \theta_{M2}^c & \cdots & \theta_{MM}^c \end{bmatrix}. \tag{12}$$

The spatial-temporal kernel function $k^x(\boldsymbol{x}_i, \boldsymbol{x}_{i'})$ can be written as the product as a spatial kernel and a temporal kernel:

$$k^x(\boldsymbol{x}_i, \boldsymbol{x}_{i'}) = k^s(p_i, q_i, p_{i'}, q_{i'}) k^t(t_i, t_{i'}), \tag{13}$$

where the spatial kernel $k^s(p_i, p_{i'}, q_i.q_{i'})$ indicates the spatial correlation, and the temporal kernel $k^t(t_i, t_{i'})$ describes the temporal correlation. Considering that the signal strengths may change differently at different directions, we utilize the commonly used anisotropic Gaussian kernel to describe the spatial correlation:

$$k^s(p_i, p_{i'}, q_i.q_{i'}) = \sigma_s^2 \text{exp}\Big(-\frac{(p_i - p_{i'})^2}{\theta_p}\Big) \text{exp}\Big(-\frac{(q_i - q_{i'})^2}{\theta_q}\Big),$$

where σ_s^2 is the maximum allowable spatial covariance. For the temporal kernel, according to the observations in Section II, it should satisfy the following two properties:

- The signal strengths at adjacent time slots are similar.
- The signal strengths at the same time of different periods

(e.g. two Mondays of different weeks) should be similar. Hence, we present a periodical kernel to describe the temporal correlation:

$$k^t(t_i, t_{i'}) = \sigma_t^2 \exp\Big(-\frac{\sin^2(\nu\pi(t_i - t_{i'}))}{\theta_t}\Big), \quad (14)$$

where σ_t^2 is the maximum allowable temporal covariance, ν is the periodical frequency. Actually, we could try other forms of kernels to describe the spatial-temporal correlations. Readers could refer to [12], [19] for more kernels of Gaussian process.

The noise of TV spectra is also an important part of the real-world measurement. Here, we consider a general Gaussian noise, where different channels have different noise variance. For example, the noise of channel ℓ is $\boldsymbol{n}_\ell \sim \mathcal{N}(0, \sigma_\ell^2)$ with σ_ℓ^2 referring to the noise variance. Thus, the kernel function (3) becomes

$$\begin{aligned} k(\boldsymbol{x}_{ij}, \boldsymbol{x}_{i'j'}, \ell, \ell') &= K^c_{\ell\ell'} k^s(p_i, p_{i'}, q_i.q_{i'}) k^t(t_j, t_{j'}) \\ &\quad + \sigma_\ell^2 \delta(\ell, \ell') \delta(\boldsymbol{x}_i, \boldsymbol{x}_{i'}), \end{aligned} \quad (15)$$

where $\delta(\ell, \ell')$ and $\delta(\boldsymbol{x}_i, \boldsymbol{x}_{i'})$ refer to the Kronecker delta function [20].

In order to avoid the redundancy in the parameters of kernels K^c, k^s, and k^t, we further let $\sigma_s^2 = \sigma_t^2 = 1$, which means the spatial kernel and temporal kernel have unit variances. The variance can be fully explained by K^c. In this way, the parameters of $k(\boldsymbol{x}_{ij}, \boldsymbol{x}_{i'j'}, \ell, \ell')$ could be denoted as

$$\boldsymbol{\theta} = \{\theta_p, \theta_q, \theta_t, \nu, \theta^c_{11}, \theta^c_{21}, \theta^c_{22}, \ldots, \theta^c_{MM}, \sigma_1^2, \sigma_2^2, \ldots, \sigma_M^2\}.$$

Given a set of training data with observations $\boldsymbol{y}_o \in \mathbb{R}^d$ and the corresponding inputs X_o, the value of $\boldsymbol{\theta}$ can be determined by maximizing the marginal likelihood $p(\boldsymbol{y}_o|X_o, \boldsymbol{\theta})$. Considering the fact that $\boldsymbol{y}_o|X_o \sim \mathcal{N}(\boldsymbol{0}, K_o)$ with K_o referring to the corresponding covariance matrix, the logarithm marginal likelihood is

$$\log p(\boldsymbol{y}_o|X_o, \boldsymbol{\theta}) = -\frac{1}{2}\log|K_o| - \frac{1}{2}\boldsymbol{y}_o^T K_o^{-1} \boldsymbol{y}_o - \frac{d}{2}\log 2\pi.$$

The logarithm marginal likelihood can be maximized by running the multivariate optimization algorithm (e.g., conjugate gradients, Nelder-Mead simplex, etc.). After the optimization, we can get the proper value of $\boldsymbol{\theta}$, the parameters of kernel function $k(\boldsymbol{x}_{ij}, \boldsymbol{x}_{i'j'}, \ell, \ell')$. Then, we can estimate the signal strengths of TV channels at different indoor locations.

C. Determining the Positions of Candidate Locations

We have shown that different positions of candidate locations would lead to different accuracies in estimation at arbitrary locations. In this part, we propose the algorithm to determine the proper positions of candidate locations, which has never been studied before. We first assume the number of candidate locations n is given, and then study how to determine a proper n.

We consider our space as a discrete set of locations $\mathcal{V}$. The possible candidate locations set $\mathcal{S}$ is thus a subset of $\mathcal{V}$: $\mathcal{S} \subset \mathcal{V}$. Now the problem becomes: find a subset $\mathcal{A}^* \subset \mathcal{S}$ with $|\mathcal{A}^*| = n$ that maximize the estimation accuracy. It is difficult to directly maximize the estimation accuracy, because we cannot give a certain mapping from the candidate locations to the estimation accuracy. Instead, we utilize the optimization criterion, proposed by Caselton and Zidek in 1984 [10], that search for $\mathcal{A}^*$ that most significantly reduce the estimation uncertainty in the rest of the space $\mathcal{V}\backslash\mathcal{A}^*$, which is equal to

$$\mathcal{A}^* = \text{argmax}_{\mathcal{A}\subset\mathcal{S}, |\mathcal{A}|=n} H(\mathcal{Y}_{\mathcal{V}\backslash\mathcal{A}}) - H(\mathcal{Y}_{\mathcal{V}\backslash\mathcal{A}}|\mathcal{Y}_{\mathcal{A}}), \quad (16)$$

where $\mathcal{A}$ is the positions of candidate locations, $\mathcal{Y}_{\mathcal{A}}$ is the set of random variables of signal strengths of all channels over the training time period at the candidate locations $\mathcal{A}$. $H(\mathcal{Y}_{\mathcal{V}\backslash\mathcal{A}})$ refers to the entropy of $\mathcal{Y}_{\mathcal{V}\backslash\mathcal{A}}$ with

$$H(\mathcal{Y}_{\mathcal{V}\backslash\mathcal{A}}) = -\int p(\boldsymbol{y}_{\mathcal{V}\backslash\mathcal{A}}) \log p(\boldsymbol{y}_{\mathcal{V}\backslash\mathcal{A}}) d\boldsymbol{y}_{\mathcal{V}\backslash\mathcal{A}}. \quad (17)$$

If $\boldsymbol{y}_{\mathcal{V}\backslash\mathcal{A}} \in \mathbb{R}^r$ obey Gaussian distribution, then

$$H(\mathcal{Y}_{\mathcal{V}\backslash\mathcal{A}}) = \frac{1}{2}\log((2\pi e)^r \text{Cov}(\boldsymbol{y}_{\mathcal{V}\backslash\mathcal{A}})), \quad (18)$$

where $\text{Cov}(\boldsymbol{y}_{\mathcal{V}\backslash\mathcal{A}})$ refers to the covariance of $\boldsymbol{y}_{\mathcal{V}\backslash\mathcal{A}}$.

Actually, the criterion $H(\mathcal{Y}_{\mathcal{V}\backslash\mathcal{A}}) - H(\mathcal{Y}_{\mathcal{V}\backslash\mathcal{A}}|\mathcal{Y}_{\mathcal{A}})$ is equivalent to the *mutual information* [21] $I(\mathcal{Y}_{\mathcal{A}}; \mathcal{Y}_{\mathcal{V}\backslash\mathcal{A}})$ between the position set $\mathcal{A}$ and the rest of space $\mathcal{V}\backslash\mathcal{A}$. Thus, equation (16) is equal to finding a set $\mathcal{A}^*$ which maximize the mutual information:

$$\mathcal{A}^* = \text{argmax}_{\mathcal{A}\subset\mathcal{S}, |\mathcal{A}|=n} I(\mathcal{Y}_{\mathcal{A}}; \mathcal{Y}_{\mathcal{V}\backslash\mathcal{A}}). \quad (19)$$

The problem of mutual information maximization has been proven to be an NP-complete problem [14]. We apply a greedy approach that determines the positions of candidate locations in sequence, choosing the position for next candidate location which provides the maximum increase in mutual information. The performance analysis of the greedy approach can be found in [14]. For the ease of presentation, we let $H(\mathcal{A}) = H(\mathcal{Y}_{\mathcal{A}})$, $\text{MI}(\mathcal{A}) = I(\mathcal{Y}_{\mathcal{A}}; \mathcal{Y}_{\mathcal{V}\backslash\mathcal{A}})$, and use $\mathcal{A} \cup \alpha$ to denote $\mathcal{A} \cup \{\alpha\}$. In this way, we determine the position of next candidate location by choosing a position α that maximize:

$$\begin{aligned} & \text{MI}(\mathcal{A} \cup \alpha) - \text{MI}(\mathcal{A}) \\ = \; & H(\mathcal{A} \cup \alpha) - H(\mathcal{A} \cup \alpha|\bar{\mathcal{A}}) - [H(\mathcal{A}) - H(\mathcal{A}|\bar{\mathcal{A}} \cup \alpha)] \\ = \; & H(\mathcal{A} \cup \alpha) - H(\mathcal{V}) + H(\bar{\mathcal{A}}) - [H(\mathcal{A}) - H(\mathcal{V}) + H(\bar{\mathcal{A}} \cup \alpha)] \\ = \; & H(\alpha|\mathcal{A}) - H(\alpha|\bar{\mathcal{A}}), \end{aligned}$$

where $\bar{\mathcal{A}} = \mathcal{V}\backslash(\mathcal{A} \cup \alpha)$.

Since $\boldsymbol{y}_\alpha|\boldsymbol{y}_{\mathcal{A}}$ and $\boldsymbol{y}_\alpha|\boldsymbol{y}_{\bar{\mathcal{A}}}$ obey Gaussian distributions whose means and covariances can be calculated based on equation (10) and equation (11), we can easily get that

$$\begin{aligned} H(\alpha|\mathcal{A}) - H(\alpha|\bar{\mathcal{A}}) &= \frac{1}{2}\log\frac{|\text{Cov}(\boldsymbol{y}_\alpha|\boldsymbol{y}_{\mathcal{A}})|}{|\text{Cov}(\boldsymbol{y}_\alpha|\boldsymbol{y}_{\bar{\mathcal{A}}})|} \\ &= \frac{1}{2}\log\frac{|K_{\alpha\alpha} - K_{\alpha\mathcal{A}}K^{-1}_{\mathcal{A}\mathcal{A}}K_{\mathcal{A}\alpha}|}{|K_{\alpha\alpha} - K_{\alpha\bar{\mathcal{A}}}K^{-1}_{\bar{\mathcal{A}}\bar{\mathcal{A}}}K_{\bar{\mathcal{A}}\alpha}|}, \end{aligned}$$

where $K_{\alpha\alpha}$ is the covariance matrix of different channels and times at position α, $K_{\alpha\mathcal{A}}$ is the covariance matrix of different channels and times between position α and positions set $\mathcal{A}$, $K_{\mathcal{A}\mathcal{A}}$ is the covariance matrix of positions set $\mathcal{A}$. $K_{\mathcal{A}\alpha}$, $K_{\alpha\bar{\mathcal{A}}}$, $K_{\bar{\mathcal{A}}\bar{\mathcal{A}}}$, and $K_{\bar{\mathcal{A}}\alpha}$ are defined in a similar way. The values of these matrices can be obtained using the kernel function k in equation (15). Actually, we can calculate the covariance matrix for the whole space $K_{\mathcal{V}\mathcal{V}}$, which contains all the needed values.

The detailed algorithm is shown in Algorithm 1. The positions of candidate locations $\mathcal{A}$ is initialized as $\mathcal{A} \leftarrow \emptyset$. Then, we iteratively choose location α^*, which maximize $\frac{|K_{\alpha\alpha} - K_{\alpha\mathcal{A}}K^{-1}_{\mathcal{A}\mathcal{A}}K_{\mathcal{A}\alpha}|}{|K_{\alpha\alpha} - K_{\alpha\bar{\mathcal{A}}}K^{-1}_{\bar{\mathcal{A}}\bar{\mathcal{A}}}K_{\bar{\mathcal{A}}\alpha}|}$, as the position of next candidate location, and add it to $\mathcal{A}$.

Intuitively, if the number of candidate locations is large

Algorithm 1: Candidate locations determination

Input : $\mathcal{V}$: discrete set of all locations,
$\mathcal{S}$: possible positions for candidate locations,
$K_{\mathcal{V}\mathcal{V}}$: covariance matrix of $\mathcal{V}$,
T_{err} error threshold.
Output: n: number of candidate locations,
$\mathcal{A}^*$: positions of candidate locations.

$n \leftarrow 0$; $\mathcal{A} \leftarrow \emptyset$;
repeat
  for $\alpha \in \mathcal{S} \backslash \mathcal{A}$ **do**
    $\eta_\alpha \leftarrow \frac{|K_{\alpha\alpha} - K_{\alpha\mathcal{A}} K_{\mathcal{A}\mathcal{A}}^{-1} K_{\mathcal{A}\alpha}|}{|K_{\alpha\alpha} - K_{\alpha\bar{\mathcal{A}}} K_{\bar{\mathcal{A}}\bar{\mathcal{A}}}^{-1} K_{\bar{\mathcal{A}}\alpha}|}$;
  $\alpha^* \leftarrow \text{argmax}_{\alpha \in \mathcal{S} \backslash \mathcal{A}}\ \eta_\alpha$;
  $n \leftarrow n + 1$; $\mathcal{A} \leftarrow \mathcal{A} \cup \alpha^*$; $\mathcal{C} \leftarrow \mathcal{V}/\mathcal{A}$;
  $\text{Cov}(\boldsymbol{y}_\mathcal{C}|\boldsymbol{y}_\mathcal{A}) \leftarrow K_{\mathcal{C}\mathcal{C}} - K_{\mathcal{C}\mathcal{A}} K_{\mathcal{A}\mathcal{A}}^{-1} K_{\mathcal{A}\mathcal{C}}$;
  $\text{Var}(\boldsymbol{y}_\mathcal{C}|\boldsymbol{y}_\mathcal{A}) \leftarrow diag(\text{Cov}(\boldsymbol{y}_\mathcal{C}|\boldsymbol{y}_\mathcal{A}))$
until $\max Var(\boldsymbol{y}_\mathcal{C}|\boldsymbol{y}_\mathcal{A}) \leq T_{err}$;
$\mathcal{A}^* \leftarrow \mathcal{A}$;
return $n, \mathcal{A}^*$;

enough, the accuracy of Step II could be satisfactory, whereas the performance of Step I is poor with large number of candidate locations. Hence, determining the number of candidate locations should consider both of the two steps. We apply a strategy that setting the number of candidate locations as small as possible while the performance of Step II is guaranteed. In this way, the performance of Step I can be satisfactory as well. In Algorithm 1, we stop adding more α^* to $\mathcal{A}$ when the estimations are accurate enough at locations $\mathcal{C} = \mathcal{V}/\mathcal{A}$. Here, we use the variance of the estimations at locations $\mathcal{C}$ as the criterion:

$$\text{Var}(\boldsymbol{y}_\mathcal{C}|\boldsymbol{y}_\mathcal{A}) = diag(\text{Cov}(\boldsymbol{y}_\mathcal{C}|\boldsymbol{y}_\mathcal{A})), \tag{20}$$

where $\text{Cov}(\boldsymbol{y}_\mathcal{C}|\boldsymbol{y}_\mathcal{A}) = K_{\mathcal{C}\mathcal{C}} - K_{\mathcal{C}\mathcal{A}} K_{\mathcal{A}\mathcal{A}}^{-1} K_{\mathcal{A}\mathcal{C}}$ is the covariance of observations over $\mathcal{C}$, and $diag(\text{Cov}(\boldsymbol{y}_\mathcal{C}|\boldsymbol{y}_\mathcal{A}))$ is the diagonal value of $\text{Cov}(\boldsymbol{y}_\mathcal{C}|\boldsymbol{y}_\mathcal{A})$. Every time we add α^* to $\mathcal{A}$, we compare the maximum value of $\text{Var}(\boldsymbol{y}_\mathcal{C}|\boldsymbol{y}_\mathcal{A})$ to a preset threshold. If the maximum value of $\text{Var}(\boldsymbol{y}_\mathcal{C}|\boldsymbol{y}_\mathcal{A})$ is larger than the threshold, we repeat the above process. Otherwise, we we stop.

D. Local Kernel and Speed Up

In the large indoor environment with many rooms and corridors, it is difficult to study a general kernel due to the complicated indoor structure caused by the indoor obstacles (e.g. walls). A common way to solve such problem is using the local kernels. This means that we could independently learn the kernel functions for different indoor areas, such as rooms and corridors, and then perform the estimation at arbitrary locations based on the corresponding kernels.

Another problem of FRISE is that the training process is very complicated since we need to measure the TV spectra not only at the candidate locations but also at the remaining indoor locations in a fine-grained way to learn the kernel functions. Besides, it seems that we need to measure the TV spectra of all locations at the same time to obtain the spatial and spectral correlations. Fortunately, the existence of the temporal correlation makes it possible to collect the training data in an asynchronous way. In this paper, we use an alternative training method with the lower complexity. We first deploy a spectrum detector at some specific location and performs a continuous measurement for a period of time (e.g. one week) to study the temporal kernel. Given the temporal kernel, we could learn the parameter of the spatial and spectral kernels based on the asynchronous measurement. Hence, we could collect the training data for spatial and spectral kernel in the same way as our asynchronous measurement in Section II-C.

Furthermore, as shown in Section II, the channels could be divided into different groups. The channels in a group are tightly correlated while the channels of different groups are almost independent. Hence, we can just consider the channels of the same group when performing the estimation. This could speed up the estimation process since we omit the useless correlations between different groups.

IV. Performance Evaluation

In this section, we extensively evaluate the performance of FRISE based real-world measurement data. We first give the setup of the evaluation and then present the evaluation results.

A. Evaluation Setup

The evaluation is based on the results of asynchronous TV spectra measurement in Section II. For the asynchronous measurement, we measure the TV channels in a lab room and a long corridor, respectively, and get 14 measurement datasets, which contain the signal strengths of 56 TV channels at different locations, in a two weeks period. We use the data of the first week to train FRISE, and use the other week's data to evaluate its performance. We choose *Estimation Error* and *White Space Error* as the evaluation criteria. Their definitions are shown as follows:

- *Estimation Error*: is the relative error between the estimation and the real value.
$$\|\hat{\boldsymbol{y}} - \boldsymbol{y}\|_2 / \|\boldsymbol{y}\|_2,$$
where $\boldsymbol{y}$ is the vector containing real signal strengths of TV channels and $\hat{\boldsymbol{y}}$ is the corresponding estimated values.
- *White Space Error*: expresses the probability that a channel is mis-identified. It is defined as the ratio between the number of channels whose status are mis-identified and the total number of channels.

To speed up the evaluation, we divided the 56 TV channels into 9 groups and run our code independently in every group.

B. Performance of Gaussian Process Based Interpolation

We compare the Gaussian process interpolation and the existing constant interpolation in estimating signal strengths of TV channels at different indoor locations. In order to present the interpolation results in an elegant way, we grid the lab room into a 20×20 grid and calculate the signal strengths of 56 TV channels at the $20 \times 20 = 400$ indoor locations. Fig. 6 illustrates an example about the interpolation results on channel 6. In Fig. 6(a), we estimate the signal strengths at the 400 grid locations based on those at the 105 measurement locations using our multitask Gaussian model. We then choose 5 locations as the candidate locations, and perform the estimation based the values at the 5 candidate locations. The result is shown in Fig. 6(b), where the candidate locations are marked by yellow points. Fig. 6(c) shows the corresponding variances of the estimations. We observe that the variances are small around the candidate locations while large at locations that are far from the candidate locations. In Fig. 6(d), we draw the constant interpolation results.

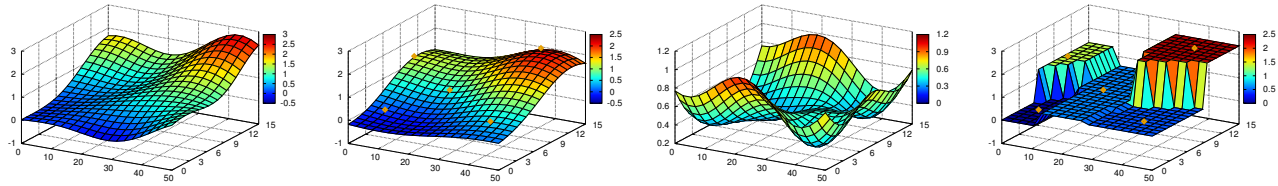

(a) Means (105 points) (b) Gaussian process interpolation (c) Estimation variance (d) Constant interpolation

Fig. 6. Estimation results.

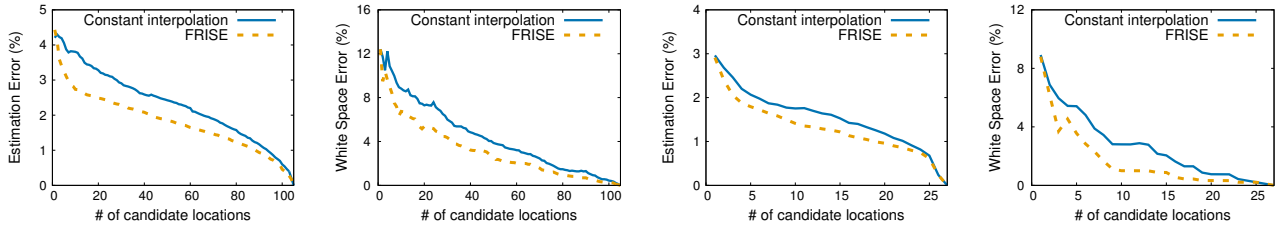

(a) Estimation error (room) (b) White space error (room) (c) Estimation error (corridor) (d) White space error (corridor)

Fig. 7. Multitask Gaussian process interpolation vs constant interpolation.

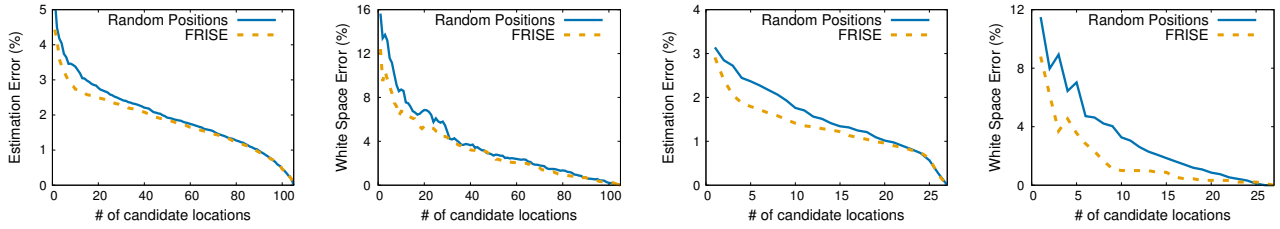

(a) Estimation error (room) (b) White space error (room) (c) Estimation error (corridor) (d) White space error (corridor)

Fig. 8. Comparison of different approaches determining the positions of candidate locations.

In Fig. 7, we compare the estimation error and white space error between multitask Gaussian process interpolation of FRISE and constant interpolation. We vary the number of the selected candidate locations from 1 to 105 (in real world we do not need so many candidate locations), and run the two interpolation algorithms based on the room data sets. The results are shown in Fig. 7(a) and Fig. 7(b). In Fig. 7(a), we observe that the estimation errors decrease as the increment of the number of candidate locations. Besides, the estimation errors of FRISE are smaller than the constant interpolation. Actually, the average estimation error is 1.90% for FRISE and 2.42% for the constant interpolation. This means that FRISE leads to an estimation error which is relatively 21.6% smaller than the constant interpolation. Fig. 7(b) demonstrates the white space errors. We observe similar results to the estimation error. The average white space error is 3.26% for FRISE, which is relatively 28.3% smaller than constant interpolation, the average white space error of which is 4.55%. Fig. 7(c) and Fig. 7(d) are the comparison results based on the data measured in the corridor. The results are similar to Fig. 7(a) and Fig. 7(b). On average, FRISE gets a relatively 15.6% smaller estimation error and a relatively 38.5% smaller white space error, compared to the constant interpolation.

C. Different Positions of Candidate Locations

We then study the performance of the mutual information based algorithm to determine the positions of the candidate locations. For the convenience of comparison, we choose the positions of the candidates among the measured indoor locations (105 in the lab room, 27 in the corridor). We compare the estimation error and the white space error between the mutual information based method and a random approach. The results are shown in Fig. 8. Fig. 8(a) and Fig. 8(b) illustrate the results based on the measured data in the lab room. We observe that both of the estimation errors and white space errors of FRISE are smaller than those of the random approach, especially when the number of candidate locations is small. On average, FRISE gets a relatively 8.2% smaller estimation error and a relatively 17.0% smaller white space error. Fig. 8(c) and Fig. 8(d) illustrate the estimation errors and the white space errors based on the data measured in the corridor. The average estimation error for FRISE is relatively 16.2% smaller than the random approach. For the white space error, this number is 47.0%. The above evaluation results show that our mutual information based method to determine the positions of the candidate locations outperforms the random approach.

Furthermore, we study the relation between the estimation variance and the number of candidate locations. We vary the number of candidate locations from 1 to 105 in the room dataset (1 to 27 for the corridor data), and calculated the maximum, average, and minimum estimation variance. The results are shown in Fig. 9. We observe that the estimation variance decrease quickly when the number of candidate

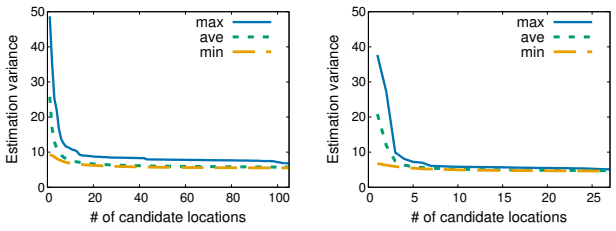

(a) room (b) corridor

Fig. 9. Estimation variance

locations is small and then change very slowly. The users can determine the proper number of candidate locations in a specific indoor space based on their maximized allowable estimation variance.

V. Related Work

As a new kind of dynamic spectrum access approach, utilizing indoor white spaces to do communications gains increasing attentions. At first, researchers mainly focused on exploring and utilizing white spaces in the outdoor scenario [22]–[25]. Then, in 2013, Ying et al. [7] discovered the problem of indoor white space exploration and proposed the first indoor white space exploration system, WISER. Then in 2015, Liu et al. [8] presented a cost efficient indoor white space exploration mechanism, called FIWEX. The two works focused on how to identify indoor white spaces. After that, Zhang et al. [26] designed an indoor white space network to efficiently utilize indoor white spaces.

Gaussian process is a Bayesian modeling technique which has been widely used in machine learning [12], queuing analysis [27], sensor networks [13], [14], and outdoor TV coverage estimation [28]. Multitask Gaussian process [17] is used to predict multiple correlated outputs, and has been applied for compiler performance analysis [16], robot inverse dynamics [29], and time series analysis [15]. However, considering the unique characteristics of indoor white spaces, the existing works of multitask Gaussian process cannot be directly applied to the indoor white space estimation. We learn a proper kernel for indoor white spaces and then propose an accurate white space estimation mechanism.

VI. Conclusion

In this paper, we have performed an indoor TV spectra measurement in a lab room and a corridor for a period of 2 weeks. The measurement results demonstrate that the constant interpolation leads to high estimation error rates and different positions of candidate locations lead to different estimation accuracies. Based on the measurement observations, we propose FRISE, which is a Fine-gRained Indoor white Space Estimation mechanism. FRISE mainly consists of a mutual information based method to determine the positions of candidate locations and a multitask Gaussian process based spatial interpolation algorithm. We evaluate the performance of FRISE based on the measurement data. The evaluation results demonstrate that FRISE leads to a maximum 38.5% less white space error compared to the constant interpolation and a maximum 47.0% less white space error compared to the estimation based on random positions of candidate locations.

References

[1] T. M. Taher, R. B. Bacchus, K. J. Zdunek, and D. Roberson, "Long-term spectral occupancy findings in chicago," in *Proc. of DySPAN*. IEEE, 2011, pp. 100–107.

[2] FCC, "FCC adopts rules for unlicensed use of TV white spaces," 2008, https://apps.fcc.gov/edocs_public/attachmatch/DOC-286566A1.pdf.

[3] S. Wang, "Cognitive communications in white space: Opportunistic scheduling, spectrum shaping and delay analysis," Ph.D. dissertation, Arizona State University, 2012.

[4] G. S. Kasbekar and S. Sarkar, "Spectrum white space trade in cognitive radio networks," in *Proc. of ITA*. IEEE, 2012, pp. 321–330.

[5] X. Feng, J. Zhang, and Q. Zhang, "Database-assisted multi-AP network on TV white spaces: Architecture, spectrum allocation and AP discovery," in *Proc. of DySPAN*. IEEE, 2011, pp. 265–276.

[6] D. Gurney, G. Buchwald, L. Ecklund, S. Kuffner, and J. Grosspietsch, "Geo-location database techniques for incumbent protection in the TV white space," in *Proc. of DySPAN*. IEEE, 2008, pp. 1–9.

[7] X. Ying, J. Zhang, L. Yan, G. Zhang, M. Chen, and R. Chandra, "Exploring indoor white spaces in metropolises," in *Proc. of MobiCom*. ACM, 2013, pp. 255–266.

[8] D. Liu, Z. Wu, F. Wu, Y. Zhang, and G. Ghen, "Fiwex: Compressive sensing based cost-efficient indoor white space exploration," in *Proc. of MobiHoc*. ACM, 2015, pp. 17–26.

[9] Y. Chen, J. Zhang, L. Yan, and M. Chen, "Exploring indoor white spaces in metropolises," in *Proc. of INFOCOM WKSHPS*. IEEE, 2015, pp. 47–48.

[10] W. F. Caselton and J. V. Zidek, "Optimal monitoring network designs," *Statistics & Probability Letters*, vol. 2, no. 4, pp. 223–227, 1984.

[11] A. J. Onwuegbuzie, L. Daniel, and N. L. Leech, "Pearson product-moment correlation coefficient," *Encyclopedia of Measurement and Statistics*, pp. 751–756, 2007.

[12] C. E. Rasmussen and C. K. I. Willians, *Gaussian Processes for Machine Learning*. http://www.gaussianprocess.org/gpml/chapters/RW.pdf, 2006.

[13] E. N. Jannah and H. Pao, "Sensor reading prediction using anisotropic kernel gaussian process regression," in *Proc. of GreenCom*. IEEE, 2014, pp. 207–214.

[14] A. Krause, A. Singh, and C. Guestrin, "Near-optimal sensor placements in gaussian processes: Theory, efficient algorithms and empirical studies," *The Journal of Machine Learning Research*, vol. 9, pp. 235–284, 2008.

[15] R. Durichen, M. Pimentel, L. Clifton, A. Schweikard, and D. A. Clifton, "Multitask gaussian processes for multivariate physiological time-series analysis," *IEEE Transactions on Biomedical Engineering*, vol. 62, no. 1, pp. 314–322, 2015.

[16] E. V. Bonilla, K. M. Chai, and C. Williams, "Multi-task gaussian process prediction," in *Proc. of NIPS*, 2007, pp. 153–160.

[17] K. Yu, V. Tresp, and A. Schwaighofer, "Learning gaussian processes from multiple tasks," in *Proc. of ICML*. ACM, 2005, pp. 1012–1019.

[18] A. Graham, "Kronecker products and matrix calculus: With applications." *JOHN WILEY & SONS, INC., 605 THIRD AVE*, 1982.

[19] C. Paciorek and M. Schervish, "Nonstationary covariance functions for gaussian process regression," *Advances in neural information processing systems*, vol. 16, pp. 273–280, 2004.

[20] E. Weisstein, "Kronecker delta function," Website, 2002, http://mathworld.wolfram.com/KroneckerDelta.html.

[21] T. M. Cover and J. A. Thomas, "Entropy, relative entropy and mutual information," *Elements of Information Theory*, pp. 12–49, 1991.

[22] S. Deb, V. Srinivasan, and R. Maheshwari, "Dynamic spectrum access in DTV whitespaces: design rules, architecture and algorithms," in *Proc. of MobiCom*. ACM, 2009, pp. 1–12.

[23] P. Bahl, R. Chandra, T. Moscibroda, R. Murty, and M. Welsh, "White space networking with Wi-Fi like connectivity," in *Proc. of SIGCOMM*. ACM, 2009, pp. 27–38.

[24] R. Vaze and C. R. Murthy, "On whitespace identification using randomly deployed sensors," in *Proc. of COMSNETS*. IEEE, 2014, pp. 1–7.

[25] T. Zhang, N. Leng, and S. Banerjee, "A vehicle-based measurement framework for enhancing whitespace spectrum databases," in *Proc. of MobiCom*. ACM, 2014, pp. 17–28.

[26] J. Zhang, W. Zhang, M. Chen, and Z. Wang, "Winet: Indoor white space network design," in *Proc. of INFOCOM*. IEEE, 2015, pp. 630–638.

[27] J. Choe and N. B. Shroff, "Use of the supremum distribution of gaussian processes in queueing analysis with long-range dependence and self-similarity," *Stochastic Models*, vol. 16, no. 2, pp. 209–231, 2000.

[28] X. Ying, C. W. Kim, and S. Roy, "Revisiting tv coverage estimation with measurement-based statistical interpolation," in *Proc. of COMSNETS*. IEEE, 2015, pp. 1–8.

[29] K. M. Chai, C. Williams, S. Klanke, and S. Vijayakumar, "Multi-task gaussian process learning of robot inverse dynamics," in *Proc. of NIPS*, 2009, pp. 265–272.